Energy xxx (xxxx) xxx

Contents lists available at ScienceDirect

Energy

journal homepage: www.elsevier.com/locate/energy

Energy storage and management system design optimization for a photovoltaic integrated low-energy building

Jia Liu [a], Xi Chen [a, b, *], Hongxing Yang [a, **], Yutong Li [c]

[a] Renewable Energy Research Group (RERG), Department of Building Services Engineering, The Hong Kong Polytechnic University, Kowloon, Hong Kong, China
[b] School of Science and Technology, The Open University of Hong Kong, Hong Kong, China
[c] Shenzhen Institute of Building Research Co., Ltd, Shenzhen, Guangdong, China

ARTICLE INFO

Article history:
Received 20 August 2019
Received in revised form
19 October 2019
Accepted 23 October 2019
Available online xxx

Keywords:
Solar photovoltaic
Battery energy storage
Energy management
Optimization
Sensitivity analysis

ABSTRACT

This study aims to analyze and optimize the photovoltaic-battery energy storage (PV-BES) system installed in a low-energy building in China. A novel energy management strategy considering the battery cycling aging, grid relief and local time-of-use pricing is proposed based on TRNSYS. Both single-criterion and multi-criterion optimizations are conducted by comprehensively considering technical, economic and environmental performances of the system based on decision-making strategies including the weighted sum and minimum distance to the utopia point methods. The single-criterion optimizations achieve superior performances in the energy supply, battery storage, utility grid and whole system aspect respectively over the existing scenario of the target building. The multi-criterion optimization considering all performance indicators shows that the PV self-consumption and PV efficiency can be increased by 15.0% and 48.6% while the standard deviation of net grid power, battery cycling aging and CO_2 emission can be reduced by 3.4%, 78.5% and 34.7% respectively. The significance and impact of design parameters are further quantified by both local and global sensitivity analyses. This study can provide references for the optimum energy management of PV-BES systems in low-energy buildings and guide the renewable energy and energy storage system design to achieve higher penetration of renewable applications into urban areas.

1. Introduction

The building sector accounts for nearly 30% of total final consumption with about three quarters of energy consumed in residential buildings [1], and the building energy demand keeps increasing at a rate of 20% between 2000 and 2017 with a great impact on the social and environmental sustainability [2]. 31% of the building energy demand is directly served by electricity, which contributes to 49% of the world electricity use [1]. Therefore, it is necessary to introduce renewable sources such as solar and wind energy for power supply to buildings to reduce its overall impact. A cumulative capacity of 505 GW solar photovoltaics (PV) [3] and 591 GW wind power [4] has been installed globally by the end of 2018, showing a remarkable rising trend in recent decades [5]. However, both solar and wind power highly depends on the weather condition, which is intermittent, unstable and unmatched with the fluctuating building load. Electrical energy storage such as battery is therefore required to store surplus renewable energy during off-peak hours and supply to electric appliances in peak time to assure a reliable power supply to buildings.

The main components of the renewable energy and electrical energy storage (RE-EES) system include the energy supply, energy storage, grid integration, load control and energy management. In terms of the energy supply, the economic performance of sizing the PV system with energy storage units is studied for residential buildings in Finland. The authors concluded that the hybrid PV-EES system can be more profitable than the standalone PV system when considering all incentives [6]. The photovoltaic-battery energy storage (PV-BES) technology is found to be economically and environmentally feasible when combined with the single diesel generator system as validated by a case study in the severe cold

* Corresponding author. Renewable Energy Research Group (RERG), Department of Building Services Engineering, The Hong Kong Polytechnic University, Kowloon, Hong Kong, China.
** Corresponding author.
E-mail addresses: climber027@gmail.com, pchen@ouhk.edu.hk (X. Chen), hongxing.yang@polyu.edu.hk (H. Yang).

https://doi.org/10.1016/j.energy.2019.116424
0360-5442/

Nomenclature

Acronyms

BES	battery energy storage
EES	electrical energy storage
EFF	efficiency
EXL	exceeded load
FIT	feed-in tariff
LCOE	levelized cost of energy
LCR	load cover ratio
NPV	net present value
NSGA-II	Non-dominated sorting genetic algorithm
PV	photovoltaic
RE	renewable energy
SCR	self-consumption ratio
SOC	state of charge
SOH	state of health
STD	standard deviation
TOU	time-of-use pricing

List of symbols

$aging_0$	initial battery aging
$aging_i$	battery aging at the current time step
Bat_{charge}	available charge capacity of battery (kWh)
$Bat_{discharge}$	available discharge capacity of battery (kWh)
Bat_{rated}	rated capacity of battery (kWh)
$C_{com\_initial}$	initial cost of each component
$C_{com\_replacement}$	replacement cost of each component
$C_{com\_residual}$	residual cost of each component
c_{ele}	grid electricity price ($/kWh)
c_{fit}	grid FIT ($/kWh)
$Charge_{\max}$	maximum charge rate of battery
c_{sub}	subsidy allowance for renewable energy generation ($/kWh)
d	discount rate
$Discharge_{max}$	maximum discharge rate of battery
E_{ele}	annual electricity from grid (kWh)
$E_{grid\ feed\text{-}in}$	feed-in electricity from PV panels into grid (kWh)
$E_{PV\ generation}$	generated electricity from PV panels (kWh)
$Equ_{lifecycle}$	equivalent life cycle number of battery
$factor_{grid\ emission}$	emission factor converting primary energy into carbon emission
f_{mai}	fixed proportion of maintenance cost to the initial cost of each component
$GE(P_{PV}, P_{load})$	PV power is not lower than building load
$Grid_{export}$	power export limit from utility grid (kW)
$Grid_{import}$	grid import limit as a ratio of rated PV power
$Grid_{optimal}$	optimal case focusing on the performance of grid relief
i	interest rate
l_{com}	lifetime of each component (year)
i_{ele}	annual increasing rate of grid electricity price
l_{sys}	lifetime of the PV-BES system (year)
$loss_{transmission}$	transmission loss of electricity power
$LT(P_{PV}, P_{load})$	PV power is lower than building load
n_{com}	number of replacement times for each component during the system service lifetime
NPV_{ele}	NPV of electricity bill ($)
NPV_{fit}	NPV of FIT ($)
NPV_{inv}	NPV of investment cost ($)
NPV_{inv_com}	investment cost of each component ($)
NPV_{inv_sys}	investment cost of the PV-BES system ($)
NPV_{mai}	NPV of maintenance cost ($)
NPV_{sub}	NPV of subsidy allowance ($)
$Pbat_i$	charging or discharging power throughout battery at the current time step (kW)
$Pbat_{net}$	net power flow through battery (kW)
$P_{battery\ to\ load}$	power from battery to building load (kW)
$P_{grid\ export}$	exported power out of utility grid (kW)
$P_{grid\ import}$	imported power into utility grid (kW)
$P_{grid\ to\ battery}$	power flow from utility grid to charge battery (kW)
$P_{grid\ to\ load}$	power flow from utility grid to meet load (kW)
P_{load}	building load demand (kW)
P_{PV}	generated power of PV panels (kW)
$P_{PV\ to\ grid}$	feed-in power from PV generator to utility grid (kW)
$P_{PV\ to\ load}$	power from PV generator to meet load (kW)
$step$	simulation time step (h)
SOC_0	initial battery state of charge
SOC_{min}	minimum state of charge of battery
SOC_i	battery state of charge at time step i
$Storage_{optimal}$	optimal case focusing on the performance of battery storage
$Supply_{optimal}$	optimal case focusing on the performance of energy supply
$System_{optimal}$	optimal case focusing on the performance of system economic-environmental impact
$Overall_{optimal}$	optimal case focusing on the overall performance of energy supply, battery storage, grid relief and system economic-environmental impact

zone of China [7]. A novel direct-couple PV model considering the PV cell number, incident radiation and temperature is developed for residential PV-BES systems and validated by laboratory tests [8]. The profitability and installation capacity of PV sharing in energy communities are researched for different building types based on the mixed-integer linear optimization algorithm. It is shown to be most profitable to install PV systems in cities with high load diversity [9]. Sizing of PV generators and technologies to improve PV energy penetrations are identified as the major focuses in the energy supply aspect of PV and energy storage systems. Different indicators on the energy supply side of the hybrid system can be further developed and combined as the optimization target to achieve a better balance.

Much attention has been paid to the energy storage unit of RE-EES systems. A PV assisted charging station using retired batteries is studied with a capacity allocation model to maximize the system net present value (NPV) based on the teaching-learning-based optimization and particle swarm optimization methods. The economic superiority of using second-use batteries for PV energy storage is illustrated against traditional batteries [10]. A novel concept of sharing the battery storage between residential consumers and local grid operators is recently developed to increase the PV penetration. This study shows a reduction of customer electricity bills and relief of the grid distribution stress [11]. Smart battery energy storage for PV systems with online controls is studied for a community in Oxford of 82 dwellings. It is shown that batteries can effectively improve the self-consumption and reduce the peak grid stress [12]. The optimal sizing of battery storage units for a net zero energy residence installed with PV systems is investigated to reduce the electricity bill and battery cost for consumers [13]. Different combinations of energy storage technologies including the battery, electric vehicle (EV), heat pump and thermal

Please cite this article as: Liu J et al., Energy storage and management system design optimization for a photovoltaic integrated low-energy building, Energy, https://doi.org/10.1016/j.energy.2019.116424

heat storage are also studied to support PV systems [14]. An innovative analytical technique is developed to optimize the total energy supply cost of PV prosumers with battery and supercapacitor storage technologies. The authors reported that the battery lifetime can be extended to 61% and the system cost can be reduced by 18% using supercapacitors [15]. It can be found that recent efforts have been made to enhance the battery storage performance by adopting the second-use battery, shared battery storage, smart battery storage and hybrid battery storage combined with other storage technologies (e.g. EV, supercapacitor). Above existing studies guide this work to consider battery aging in the system design and optimization to extend the battery lifecycle and reduce the system cost.

Rising PV penetrations in buildings also bring a great burden to the utility grid, so that efforts have been made to integrate the utility grid with RE-EES systems. The economic performance of the distributed RE-EV system is analyzed with different coordination strategies. It is indicated that the vehicle to grid strategy is cost-effective for fully using EV batteries [16]. The vehicle to grid strategy is also reported to be effective in providing primary frequency control and dynamic grid support [17]. The technical and economic performance of a household PV-BES system in Norway is studied considering the grid power limit, showing that the building integrated PV system with battery storage has good performance under the monthly grid power limits [18]. The optimal integration of PV systems with the utility grid is explored with a grid model of 352 buses and 441 lines in Japan to minimize the system cost [19]. An optimization is conducted on a PV-BES system considering the relationship of the self-sufficiency, financial incentive and grid integration, suggesting that grid operators should adjust guidelines for PV-BES systems and adopt feed-in limitations [20]. Effective methods are developed to facilitate the grid support to reduce its burden when connected with RE-EES systems such as grid integration with energy supply and storage, setting grid power limit and providing governmental incentives. The grid integration will also be considered in this work by proposing grid export and import limits, where the standard deviation of the net grid power is derived to minimize the average grid stress.

Furthermore, load controls can contribute to a higher system efficiency and feasibility as targeted by many researchers. The demand side management of the RE-EES system in micro-grid networks is investigated to improve the system stability and reduce the grid pressure. The game theory method based on blockchain technologies is proposed as an effective modelling tool to support the increasing building demand [21]. The solar plus model combining the load control on PV systems with energy storage units is optimized considering the smart hot water heater and air conditioner. The simulation results reveal that the solar plus model is able to achieve economic benefits under different rate contexts [22]. The authors also reviewed the end-user economics of the solar plus model in domestic buildings and reported that load control appliances are more profitable than batteries in the current cost [23]. Existing studies on the demand response of renewable energy systems are found to be focusing on smart appliances to shift the load for a better match with the renewable energy generation.

In addition, an increasing attention has been focused on the energy management component, which is deemed a vital aspect of RE-EES systems to supervise the power flow. A three-stage feed-in scheduling method is developed for the PV system with battery and electrolyzer storage units to improve the system flexibility. It shows that the proposed method is both technically and economically feasible based on the comparative analysis [24]. NPV of the PV system with the second-use battery is evaluated based on two energy management strategy models including increasing self-consumption only and increasing self-consumption with load-leveling [25]. The energy management strategy for residential PV-BES systems is also developed considering the matching of thermostatically controlled demand and battery charging. The case study shows that the system energy consumption is reduced by 30% while maintaining the power supply quality and extending the battery lifecycle [26]. The energy management algorithm is proposed for an on-grid PV system with battery and supercapacitor units considering dynamic changes of the cloud condition and load power, as validated to be feasible by a prototype experiment [27]. Moreover, a predictive management for a PV system with heat pump and battery units is developed based on the two-stage stochastic programming and rule-based control, where the operational cost is lowered by 4.5% [28]. Different energy management algorithms have been developed for RE-EES systems to supervise the system power flow with various targets such as improving system flexibility, reducing system cost and extending battery lifecycle. Based on these management algorithms and targets, this study proposes an innovative energy management strategy considering the battery cycling aging, grid relief and local time-of-use pricing through a joint modeling platform of TRNSYS and jEPlus + EA to improve and optimize the PV-BES system installed in a real building.

Although much attention has been paid to RE-EES systems, few efforts have been made to explore practical applications in China, especially in the system scale-up. Moreover, few studies have thoroughly investigated the comprehensive technical, economic and environmental optimization of the coupled energy conversion and storage system. To fill such research gaps, a study on the energy storage and management system design optimization for a PV integrated low-energy building is conducted. The original contribution of this study lies in the following aspects: (1) A novel energy management strategy considering the battery cycling aging, grid relief and local time-of-use pricing is proposed based on a joint modeling platform of TRNSYS and jEPlus + EA to optimize the PV-BES system installed in a practical low-energy building located in the hot-summer and warm-winter region of China. (2) Both single-criterion and multi-criterion optimizations are conducted by comprehensively considering the technical, economic and environmental performances of the energy supply, battery storage, utility grid and whole system based on decision-making strategies including the weighted sum and minimum distance to the utopia point methods. The battery size and grid relieving parameters including the grid export limit and grid import limit are optimized for multiple performance criteria. (3) Both local and global sensitivity analyses are conducted to further quantify the significance and impact of selected design parameters in order to provide guidance on the system design and management for the low-energy building. Research findings in this work can be used as references for the RE-EES system design to achieve a greater penetration of renewable energy into urban areas.

2. Methodology

As shown in Fig. 1, this study aims to explore an optimum energy management strategy for the PV-BES system for a real low-energy building in Shenzhen, as the existing management strategy (see Case 1) cannot make full use of the energy conversion and storage system. The PV energy utilization is low with a high system cost because surplus PV power is not fed into the utility grid to gain the local PV feed-in tariff (FIT) incentive and a fixed grid pricing scheme is applied to the existing building. The existing operation scenario is therefore modelled as the baseline case for comparison.

In order to improve the existing system performance, Case 2 is first proposed based on the same system configuration with Case 1 but a new control strategy considering the grid feed-in and time-of-

Please cite this article as: Liu J et al., Energy storage and management system design optimization for a photovoltaic integrated low-energy building, Energy, https://doi.org/10.1016/j.energy.2019.116424

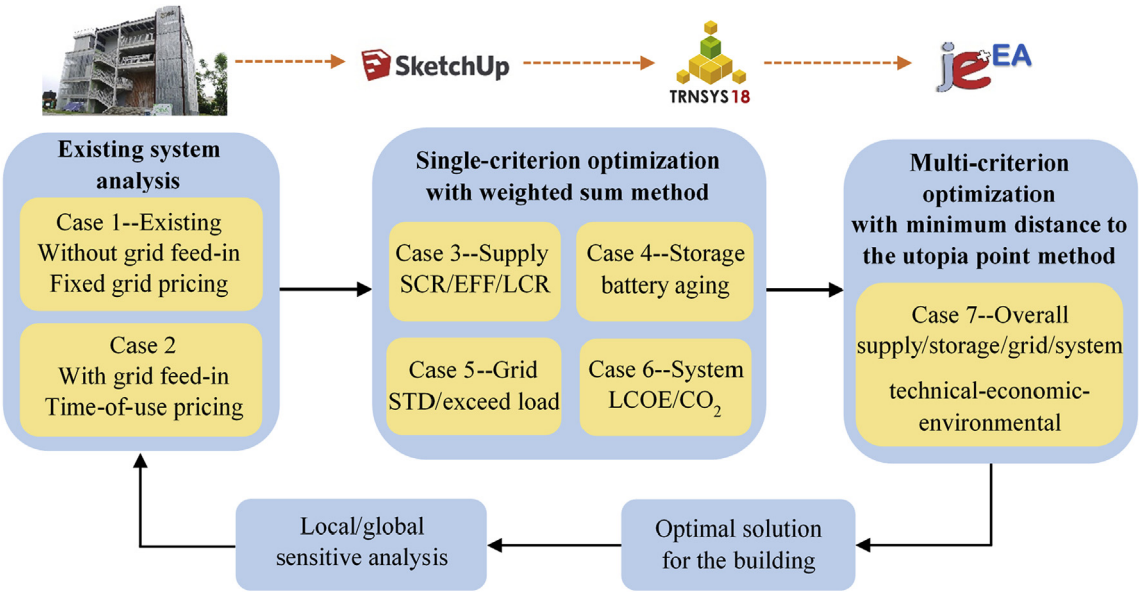

Fig. 1. Proposed framework of optimization on the PV-BES system in the low-energy building.

use pricing. On top of Case 2, both single-criterion and multi-criterion optimizations are conducted with three optimization variables: the battery cell number, grid export limit, and grid import limit. The optimization analyses are conducted on the joint modeling and optimization platform of TRNSYS and jEPlus + EA with the Non-dominated sorting genetic algorithm (NSGA-II) at a simulation time step of 0.125 h. Regarding the optimization design and objectives, single-criterion optimizations (Case 3–6) with the weighted sum method are performed focusing on four major aspects of the PV-BES system including the energy supply, battery storage, utility grid and whole system. Case 3 aims to optimize the supply performance with a combined objective of three indicators including the PV self-consumption ratio (SCR), PV power efficiency (EFF) and load cover ratio (LCR). Case 4 focuses on the battery health by minimizing the battery cycling aging. Case 5 explores the grid relief potential to minimize the standard deviation (STD) of the net grid power and reduce the exceeded load. Case 6 intends to achieve good economic and environmental system performances considering the levelized cost of energy (LCOE) and CO_2 emission. Then, the multi-criterion optimization is performed with the minimum distance to the utopia point method in Case 7 focusing on the overall performance of above four aspects for a comprehensive technical, economic and environmental evaluation of the PV-BES system. Finally, local sensitivity analyses based on the optimal solution and global sensitivity analyses with the Fourier Amplitude Sensitivity Test (FAST) are conducted to further quantify the significance and impact of selected design parameters.

2.1. Photovoltaic-battery energy system in the low-energy building

The low-energy building is located in Shenzhen of China with a hot and humid climate, and it is mainly designed for office and exhibition functions. Fig. 2 shows the appearance of the building installed with the PV-BES system and energy management center. The total building area is 658.15 m^2 with 3 floors and the detailed as-built parameters are shown in Table 1.

In terms of the PV-BES system, thin-film PV panels are used with a total rated capacity of 13.12 kW and a battery bank with a rated capacity of 45.6 kW h is installed. The detailed specification of the PV-BES system is shown in Table 2.

Fig. 2. Low-energy building installed with the PV-BES system in Shenzhen.

2.2. Photovoltaic-battery energy storage system modelling

Fig. 3 shows the schematic of the developed PV-BES model based on the TRNSYS platform, where five main components, namely the building load, PV panel, battery storage, utility grid, and energy management strategy are integrated.

2.2.1. Building component

A SketchUp model of the building is firstly established according to practical building dimensions and then imported into TRNSYS to define internal building properties. According to the practical building configuration, the load is calculated with submodules of the building envelope, ventilation, air conditioning, indoor occupant, equipment and lighting based on Type 56, Type 117, Type 752, Type 655, Type 648 and other auxiliary components in the TRNSYS library [32]. The typical meteorological year weather data of Shenzhen is connected to the building and PV generators [33].

2.2.2. Photovoltaic component

Both rooftop and façade PV panels are modelled according to

Please cite this article as: Liu J et al., Energy storage and management system design optimization for a photovoltaic integrated low-energy building, Energy, https://doi.org/10.1016/j.energy.2019.116424

Table 1
Thermal properties of the low-energy building.

Building	Parameter	Value
Roof	Heat transfer coefficient	0.30 W/(m^2·K)
	Thermal inertia index	1.07
External-wall	Heat transfer coefficient	0.43 W/(m^2·K)
	Thermal inertia index	2.78
External-window	Window-wall ratio	East: 0.47; South: 0.59; West: 0.45; North: 0.40
	Heat transfer coefficient W/(m^2·K)	East: 2.64; South: 2.38; West: 2.14; North: 2.51
	Shading coefficient	East: 0.30; South: 0.22; West: 0.16; North: 0.26
Lighting	Office power density	5.80 W/m^2
	Laboratory power density	7.70 W/m^2
	Corridor power density	2.50 W/m^2
	Convective heat transfer ratio	0.33 [29]
	Radiant heat transfer ratio	0.67 [29]
Occupant [29]	Sensible heat	66 W/person
	Latent heat	68 W/person
	Convective heat transfer ratio	0.4
	Radiant heat transfer ratio	0.6
Equipment [29]	Office power density	15 W/m^2
	Laboratory power density	15 W/m^2
	Corridor power density	5 W/m^2
	Convective heat transfer ratio	0.3
	Radiant heat transfer ratio	0.7

Table 2
Specification of the PV-BES system.

Solar panel	ASP-S1-80 W (CdTe)
Maximum power	80 W
Open circuit voltage	118.5 V
Short circuit current	1.01 A
Voltage at max. power point	92 V
Current at max. power point	0.88 A
Maximum system voltage	1000 V
Rooftop cell number	149
Façade PV cell number	15
Battery	**NP100-12FR (Lead-Acid)**
Nominal capacity	100 Ah/12 V
Number in series	38
Operational *SOC* (SOC_{min}-SOC_{max})	25%–90% [30]
Max. charging/discharging rate	0.2C
Charging efficiency	0.9
Life cycle	1000 cycles [31]

practical building installations. TRNSYS determines the current-voltage characteristic of the rooftop PV array using the empirical equivalent circuit model [34,35]. The power generation of the PV system is the product of the current and voltage under the maximum power point tracking mode to achieve higher energy efficiency. The building integrated PV model Type 567 is adopted to model façade PV panels integrated with the multi-zone building model Type 56, which is developed from Duffie and Beckman's thermal algorithm [35].

2.2.3. Battery component

The battery model is developed based on the energy balance with the state of charge (*SOC*) as the iteration indicator shown in Eq. (1) [8]:

$$SOC_i = SOC_0 + \frac{\int Pbat_{net}}{Bat_{rated} \cdot SOH} \tag{1}$$

where SOC_0 is the initial battery state of charge; $Pbat_{net}$ is the net power flow through the battery bank including charging and discharging power in opposite values, kW; Bat_{rated} is the rated capacity of the battery bank, kWh; *SOH* is the battery state of health considering the battery degradation. In this study, only cycling aging of the battery tank is considered as shown in Eq. (2) [36,37]:

$$cycling\ aging_i = aging_0 + 0.5 \cdot \frac{\int |Pbat_i|}{Bat_{rated}} \cdot \frac{1}{Equ_{lifecycle}} \tag{2}$$

where $aging_0$ is the initial battery aging; $Pbat_i$ is the charging or discharging power throughout the battery bank, kW; $Equ_{lifecycle}$ is the equivalent life cycle number of the battery bank degrading from its initial full useable capacity at 100% *SOH* to the end of its life at 80% *SOH*. The lead-acid battery in the building normally has 1000 cycles in its service life [31]. It is assumed that battery *SOH* is at 80% when battery aging arrives at 1, so the battery *SOH* can be formulated as Eq. (3) [36,37]:

$$SOH_i = SOH_{i-1} - aging_i \cdot 0.2 \tag{3}$$

2.2.4. Grid component

For the grid, STD of the net grid power is derived to show the average grid stress as per Eq. (4) [38]:

$$Average grid stress_{year} = STD\left(P_{grid to load} + P_{grid to battery} - P_{PV to grid}\right)_{step} \tag{4}$$

where $P_{grid\ to\ load}$ is the power flow from the utility grid to meet the load, kW; $P_{grid\ to\ battery}$ is the power flow from the utility grid to charge the battery bank, kW; $P_{PV\ to\ grid}$ is the feed-in power from the PV generator to the utility grid, kW.

In order to further consider the grid integration with the PV-BES system, both grid export and import limits are introduced to this model. The grid export limit ($Grid_{export}$) is set to regulate the grid to meet the load and battery demand, while the exceeded load over the $Grid_{export}$ in Eq. (5) will still be met by the utility grid. Exceeded battery demand, however, will not be addressed.

$$P_{exceeded\ load} = P_{load} - P_{PV\ to\ load} - P_{battery\ to\ load} - Grid_{export} \tag{5}$$

where P_{load} is the building load demand, kW; $P_{PV\ to\ load}$ is the power from PV generators to meet the load, kW; $P_{battery\ to\ load}$ is the power

Please cite this article as: Liu J et al., Energy storage and management system design optimization for a photovoltaic integrated low-energy building, Energy, https://doi.org/10.1016/j.energy.2019.116424

from the battery bank to the building load, kW.

The grid import limit ($Grid_{import}$), which is the ratio of the rated PV power, is set to limit surplus PV power feeding into the utility grid so that any power over the $Grid_{import}$ is dumped. These grid integration indicators are subject to design optimizations as an original contribution of this research.

$$P_{grid\ to\ battery} = min\Big(Grid_{export} - (P_{load} - P_{PV}),\ Bat_{charge}\Big)\cdot LT(P_{PV}, P_{load}) + min\Big(Grid_{export},\ Bat_{charge} - (P_{PV} - P_{load})\cdot GE(P_{PV}, P_{load})\Big) \quad (13)$$

2.2.5. Energy management component

This study aims to improve the overall performance of the PV-BES system considering the supply efficiency, battery health, grid integration and system economic-environmental impact by developing a new energy management strategy as shown in Fig. 4.

When PV power is available, it is firstly supplied to meet the building load as shown in Eq. (6):

$$P_{PV\ to\ load} = min(P_{PV},\ P_{load}) \quad (6)$$

where P_{PV} is the generated power of PV panels considering an inverter efficiency of 0.95, kW; P_{load} is the building load demand, kW.

Then the power flow is directed according to peak-valley hours in the day. During valley hours in weekdays, surplus PV power after meeting the load is used to charge the battery as shown in Eq. (7) with a charging efficiency of 0.9:

$$P_{PV\ to\ battery} = min\Big((P_{PV} - P_{load}),\ Bat_{charge}\Big) \quad (7)$$

where Bat_{charge} is the available charge capacity of the battery bank formulated as Eq. (8):

$$Bat_{charge} = max((SOC_{max} - SOC)\cdot Bat_{rated}\cdot SOH \Big/ step,\ Charge_{max}\cdot Bat_{rated}\cdot SOH\Big) \quad (8)$$

where Bat_{rated} is the rated capacity of the battery bank, kWh; *step* is the simulation time step (0.125 h); $Charge_{\max}$ is the maximum charge rate of the lead-acid battery in the targeted building (0.2C).

Then surplus PV power after meeting the load and battery is fed into the utility grid and gets FIT allowance as shown in Eq. (9):

$$P_{PV\ to\ grid} = min\Big(Grid_{import}\cdot PV_{rated},\ P_{PV} - P_{load} - Bat_{charge}\Big) \quad (9)$$

where $Grid_{import}$ is the grid import limit as a ratio of rated PV power PV_{rated}. If surplus PV power exceeds the grid import limit, the exceeded part will be dumped as per Eq. (10):

$$P_{PV\ dumped} = max\Big(0,\ P_{PV} - P_{load} - Bat_{charge} - Grid_{import}\cdot PV_{rated}\Big) \quad (10)$$

If PV power is not enough for the building load or battery, the utility grid will meet both the load and battery demand given the low grid price in valley hours as per Eqs. (11)–(13):

$$P_{grid\ to\ load} = min(Grid_{export},\ P_{load} - P_{PV}) \quad (11)$$

where $Grid_{export}$ is the power export limit from the utility grid, kW. It should be noted that the exceeded load (See Eq. (12)) with reference to $Grid_{export}$ will still be met by the grid, but the exceeded battery demand will not be met by the grid.

$$P_{exceeded\ load} = max(0,\ P_{load} - P_{PV} - Grid_{export}) \quad (12)$$

where $LT(P_{PV}, P_{load})$ means the PV power is lower than the building load and the grid will meet both the unsatisfied load and battery. And $GE(P_{PV}, P_{load})$ means the PV power is not lower than the building load so that the battery can be charged by both PV and grid.

During flat hours with a relatively high grid electricity price, the grid will not be used to charge the battery even when surplus PV power after meeting the building load is not enough for charging the battery. And during peak hours with the highest grid electricity price, the battery will take precedence over the grid to meet the unsatisfied load from PV power as shown in Eq. (14):

$$P_{battery\ to\ load} = min\Big(P_{load} - P_{PV}, Bat_{discharge}\Big) \quad (14)$$

where $Bat_{discharge}$ is the available discharge capacity of the battery as per Eq. (15):

$$Bat_{discharge} = max((SOC - SOC_{min})\cdot Bat_{rated}\cdot SOH \Big/ step,\ Discharge_{max}\cdot Bat_{rated}\cdot SOH\Big) \quad (15)$$

where $Discharge_{max}$ is the maximum discharge rate of the lead-acid battery in the building (0.2C).

As the building is not in operation during weekends, PV power will firstly be used to charge the battery and then fed into the utility grid. And residual PV power over the grid import limit will be dumped.

2.3. Optimization of system design and management

Single-criterion and multi-criterion optimizations are conducted considering the technical, economic and environmental performances of the PV-BES system with the joint TRNSYS and jEPlus + EA platform.

2.3.1. Optimization objectives

Eight optimization objectives are established under four major aspects of the PV-BES system including the energy supply, battery storage, utility grid and whole system as shown in Fig. 5. For the energy supply aspect, three indicators including SCR, EFF and LCR are combined as the performance criterion. For the battery storage aspect, the annual battery cycling aging is the only focus. And for the utility grid aspect, two indicators including STD of net grid power and the exceeded load are integrated as the criterion. And for the whole system aspect, LCOE and CO_2 emission are synthesized as the whole system performance criterion.

For the energy supply aspect, SCR is formulated as Eq. (16) [39]:

Please cite this article as: Liu J et al., Energy storage and management system design optimization for a photovoltaic integrated low-energy building, Energy, https://doi.org/10.1016/j.energy.2019.116424

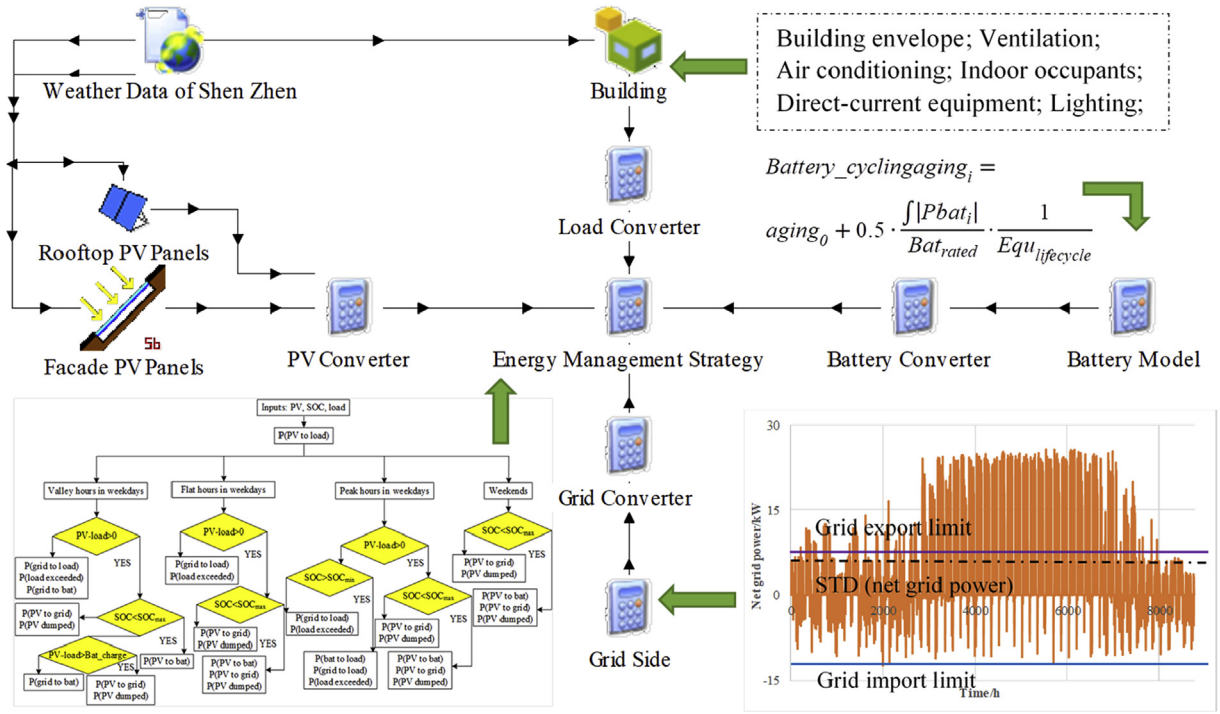

Fig. 3. Simulation model of the PV-BES system in TRNSYS environment.

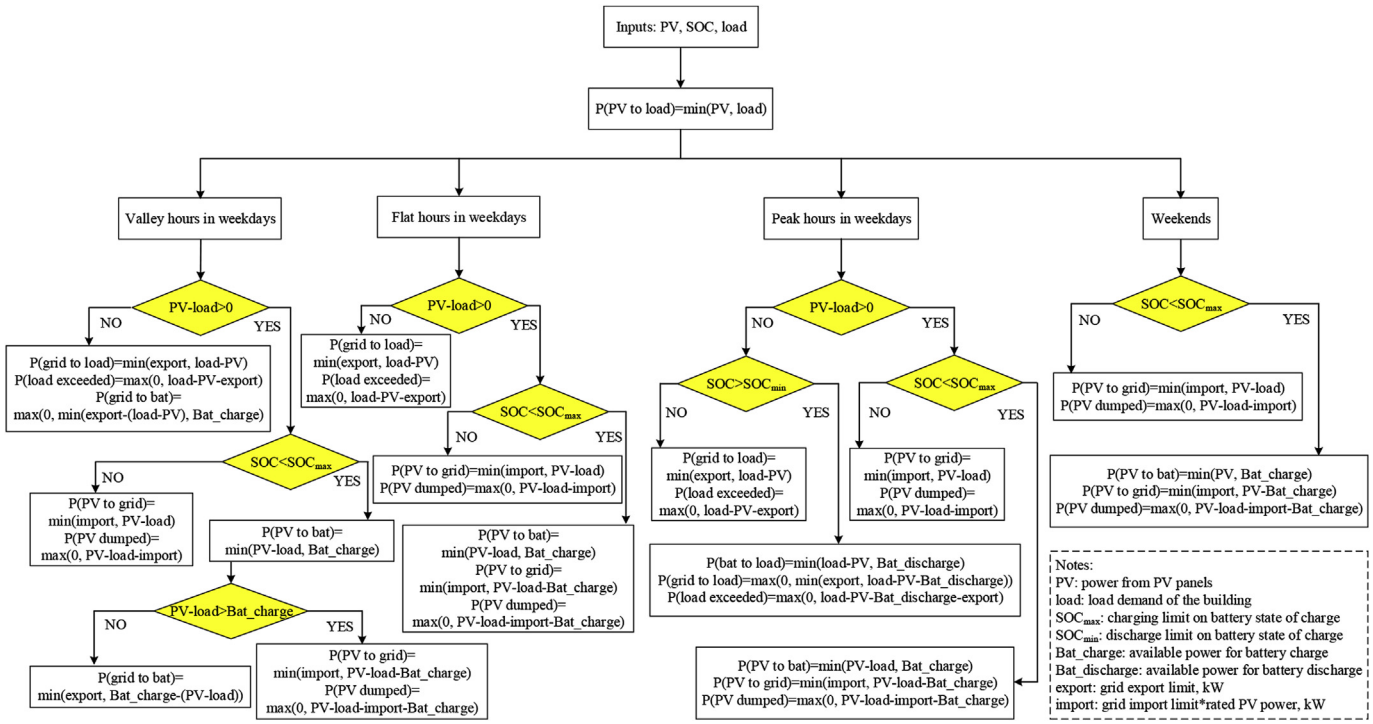

Fig. 4. Proposed energy management strategy of the PV-BES system for the low-energy building.

$$PV\ self-consumption\ ratio = \frac{self-consumed\ PV\ electricity}{total\ electricity\ generation\ from\ PV} = \frac{E_{pv\ to\ load} + E_{pv\ to\ battery}}{E_{pv}} \quad (16)$$

Since some PV power may be dumped when exceeds the grid import limit, efficiency of the PV generator is also assessed as per Eq. (17):

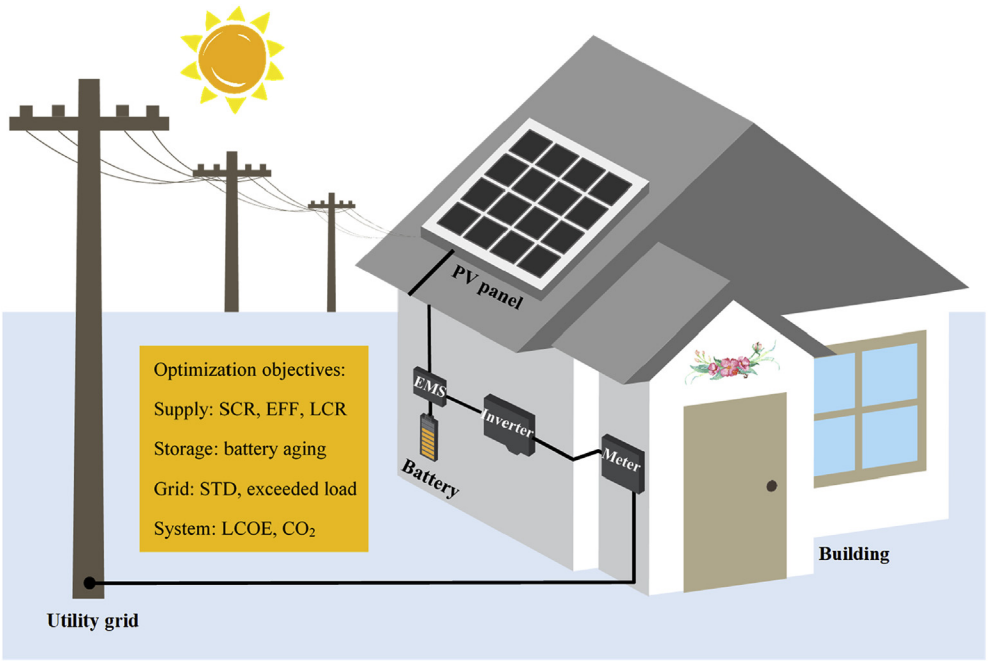

Fig. 5. Optimization objectives of the PV-BES system.

$$PV\ efficiency = \frac{utilized\ PV\ electricity}{total\ electricity\ generation\ from\ PV} = \frac{E_{pv\ to\ load} + E_{pv\ to\ battery} + E_{pv\ to\ grid}}{E_{pv}} \quad (17)$$

In order to evaluate the load matching of the PV-BES system, LCR of the PV-BES system is presented as shown in Eq. (18). It should be noted that the battery bank can be charged by the low-price grid power.

$$load\ cover\ ratio = \frac{PV - BES\ system\ provided\ electricity}{total\ electricity\ demand} = \frac{E_{pv\ to\ load} + E_{battery\ to\ load}}{E_{load}} \quad (18)$$

For the battery storage side, the annual cycling aging is calculated as explained in Eq. (2). For the utility grid side, STD of the net grid power is calculated to evaluate the average grid stress as shown in Eq. (19), and EXL is expressed by Eq. (20):

Table 3
Parameters for economic analysis of the PV-BES system.

Parameter		Value
PV system	Initial cost ($c_{pv\_initial}$)	1400 $/kW
	Life time (l_{pv})	20 years
Battery system	Initial cost ($c_{bat\_initial}$)	150 $/kWh
	Life time ($l_{battery}$)	5 years
Inverter	Initial cost ($c_{inverter\_initial}$)	90 $/kW
	Life time ($l_{inverter}$)	10 years
Grid FIT (c_{fit})		0.058 $/kWh [40]
Governmental subsidy (c_{sub})		0.014 $/kWh [40]
Discount rate (d)		4.5%/year [41]
Interest rate (i)		5.8%/year [41]
Electricity price (c_{ele})		See Table 4
Electricity price rising rate (i_{ele})		1.85%/year [42]
Life time of PV-BES system (l_{sys})		20 years

$$Averagegridstress_{year} = STD\left(P_{gridtoload} + P_{gridtobattery} - P_{PVtogrid}\right)_{step} \quad (19)$$

$$Exceeded\ load = P_{load} - P_{PV\ to\ load} - P_{battery\ to\ load} - Grid_{export} \quad (20)$$

For the whole system aspect, LCOE and CO_2 emission are considered. In order to calculate the system LCOE, NPV is firstly evaluated as shown in Eq. (21):

$$NPV_{sum} = NPV_{inv} + NPV_{mai} + NPV_{ele} + NPV_{sub} + NPV_{fit} \quad (21)$$

where NPV_{inv} is NPV of the system investment cost, $; NPV_{mai} is NPV of the maintenance cost, $; NPV_{ele} is NPV of the electricity bill, $; NPV_{sub} is NPV of the subsidy allowance, $; NPV_{fit} is NPV of FIT, $.

The system investment cost (NPV_{inv_sys}) includes those of the PV panels, battery cells and inverters as summarized by Eq. (22):

$$NPV_{inv\_sys} = \sum NPV_{inv\_com} = NPV_{inv\_PV} + NPV_{inv\_battery} + NPV_{inv\_inverter} \quad (22)$$

And the investment cost of each component (NPV_{inv_com}) consists of the initial cost ($C_{com\_initial}$), replacement cost ($C_{com\_replacement}$) and residual cost ($C_{com\_residual}$) as shown in Eqs. (23)–(25):

$$NPV_{inv\_com} = C_{com\_initial} + C_{com\_replacement} - C_{com\_residual} \quad (23)$$

$$C_{com\_replacement} = C_{com\_initial} \cdot \sum_{n=1}^{n_{com}} \frac{(1-d)^{n \cdot l_{com}}}{(1+i)^{n \cdot l_{com}}} \quad (24)$$

$$C_{com\_residual} = C_{com\_initial} \cdot \frac{l_{com} - mod(l_{sys}, l_{com})}{l_{com}} \cdot \frac{(1-d)^{l_{sys}}}{(1+i)^{l_{sys}}} \quad (25)$$

where n_{com} is the number of replacement times for each

Table 4
Electricity price of the utility grid in different period [43].

Price mode	Time	Hours	Price ($/kWh)
Time-of-use pricing	Valley period	23:00–7:00	0.04
	Flat period	7:00–9:00, 11:30–14:00, 16:30–19:00, 21:00–23:00	0.10
	Peak period	9:00–11:30, 14:00–16:30, 19:00–21:00	0.15
Fixed pricing	All period	0:00–24:00	0.10

Table 5
Optimization parameters.

Parameter	Value	
Population size	10 [46]	
Maximum generation	200	
Crossover probability	0.9 [47]	
Mutation probability	0.05 [47]	
Tournament size	2	
Variable	Range	Increment
Battery cell number	2–100	2 cells
Grid export limit	0–30 kW	1 kW
Grid import limit (ratio of rated PV power)	0–1	0.1

component during the system service lifetime; l_{com} is the lifetime of each component, year; l_{sys} is the lifetime of the PV-BES system, year; d is the discount rate; i is the interest rate; and detailed values are summarized in Table 3.

The system maintenance cost is assumed to be proportional to the initial cost (fixed proportion f_{mai}) of each component as shown in Eq. (26):

$$NPV_{mai\_com} = f_{mai} \cdot C_{com\_initial} \cdot \frac{(1+i)^{l_{sys}} - 1}{(1+i)^{l_{sys}} \cdot i} \tag{26}$$

The cost of buying electricity from the utility grid is shown in Eq. (27):

$$NPV_{ele} = c_{ele} \cdot E_{ele} \cdot \left(\sum_{l=1}^{l_{sys}} \frac{(1+i_{ele})^{l-1}}{(1+i)^{l-1}} \right) \tag{27}$$

where i_{ele} is the annual increasing rate of the grid electricity price (c_{ele}); and the annual electricity from the grid (E_{ele}) is assumed to be unchanged.

According to the local regulation of renewable energy applications in buildings, both the subsidy and FIT can be harvested by the PV-BES system. Compared with NPV value of above items, reimbursement from the system subsidy and grid FIT is the benefit in negative value. And it is assumed that the subsidy allowance (c_{sub}) keeps the same during the system service lifetime, and FIT cost (c_{fit}) increases with the grid electricity price. So NPV of the subsidy and FIT can be formulated as Eqs. (28) and (29):

$$NPV_{sub} = -c_{sub} \cdot E_{PV\ \ generation} \cdot \sum_{l=1}^{l_{sys}} \frac{1}{(1+i)^{l-1}} \tag{28}$$

where $E_{PV\ generation}$ is the generated electricity from PV panels, kWh.

$$NPV_{fit} = -c_{fit} \cdot E_{grid\ feed-in} \cdot \sum_{l=1}^{l_{sys}} \frac{(1+i_{ele})^{l-1}}{(1+i)^{l-1}} \tag{29}$$

where $E_{grid\ feed\text{-}in}$ is the feed-in electricity from PV panels into the utility grid, kWh.

Therefore, the system *LCOE* can then be calculated by Eq. (30):

$$LCOE = \frac{NPV_{sum} \cdot \frac{(1+i)^{l_{sys}} \cdot i}{(1+i)^{l_{sys}} - 1}}{\int P_{load}} \tag{30}$$

The annual CO_2 emission can be formulated as Eq. (31) [41].

$$CO_2\ emission = \left(\int P_{grid\ export} - \int P_{grid\ import} \right) \times loss_{transmission} \times factor_{grid\ emission} \tag{31}$$

where $P_{grid\ export}$ is the exported power out of the utility grid, kW; $P_{grid\ import}$ is the imported power into the utility grid, kW; $loss_{transmission}$ is the transmission loss of the electricity power (10%); $factor_{grid\ emission}$ is the emission factor converting the primary energy into the carbon emission (0.238 tCO_2/MWh) [41].

2.3.2. Optimization methods

NSGA-II is applied to solve above multi-objective optimizations given its high efficiency [41]. Pareto-optimal solutions are derived from the non-dominated population sorting strategy under existing optimization constraints and settings within a specified number of model evaluations [44]. In each evaluation, the crowding distance is calculated based on the initial population sorting and used to find the fittest solution along with the tournament selection. Crossovers and mutations are performed to ensure a comprehensive and converged searching of the problem space [41,45]. The optimization parameter is shown in Table 5.

The optimization process performs with the jEPlus + EA platform, which combines the TRNSYS model with NAGA-II. In order to obtain a single-criterion optimum solution in Case 3–6 focusing on the energy supply, battery storage, utility grid, and whole system performance criterion respectively, the weighted sum method [48]

Table 6
Optimization criteria of optimization cases.

Optimization case		Optimization criterion
Single-criterion optimization	Case 3:	$Supply_{optimal} = \frac{1}{3}\frac{SCR - SCR_{min}}{SCR_{max} - SCR_{min}} + \frac{1}{3}\frac{EFF - EFF_{min}}{EFF_{max} - EFF_{min}} + \frac{1}{3}\frac{LCR - LCR_{min}}{LCR_{max} - LCR_{min}}$
	Case 4:	$Storage_{optimal} = \frac{aging - aging_{min}}{aging_{max} - aging_{min}}$
	Case 5:	$Grid_{optimal} = \frac{1}{2}\frac{STD - STD_{min}}{STD_{max} - STD_{min}} + \frac{1}{2}\frac{EXL - EXL_{min}}{EXL_{max} - EXL_{min}}$
	Case 6:	$System_{optimal} = \frac{1}{2}\frac{LCOE - LCOE_{min}}{LCOE_{max} - LCOE_{min}} + \frac{1}{2}\frac{CO_2 - CO_{2\ min}}{CO_{2\ max} - CO_{2\ min}}$
Multi-criterion optimization	Case 7:	$Overall_{optimal} = [Supply_{optimal}, Storage_{optimal}, Grid_{optimal}, System_{optimal}]^T$

Please cite this article as: Liu J et al., Energy storage and management system design optimization for a photovoltaic integrated low-energy building, Energy, https://doi.org/10.1016/j.energy.2019.116424

Table 7
Optimization results of studied cases.

Case	Case 1 (building existing)	Case 2 (grid feed-in and TOU)	Optimization				
			Case 3 (supply)	Case 4 (storage)	Case 5 (grid)	Case 6 (system)	Case 7 (overall)
Time-of-use pricing (TOU)	_	✓	✓	✓	✓	✓	✓
Supply optimal (max. SCR, EFF and LCR)	_	_	✓	_	_	_	✓
Storage optimal (min. battery aging)	_	_	_	✓	_	_	✓
Grid optimal (min. STD and exceeded load)	_	_	_	_	✓	_	✓
System optimal (min. LCOE and CO_2 emission)	_	_	_	_	_	✓	✓
Optimization parameters							
Battery cell number	38	38	100	100	28	2	90
Grid export limit/kW	30	30	5	0	30	1–30	5
Grid import limit (ratio of PV rated power)	0	1	1	0–1	0	1	0.8

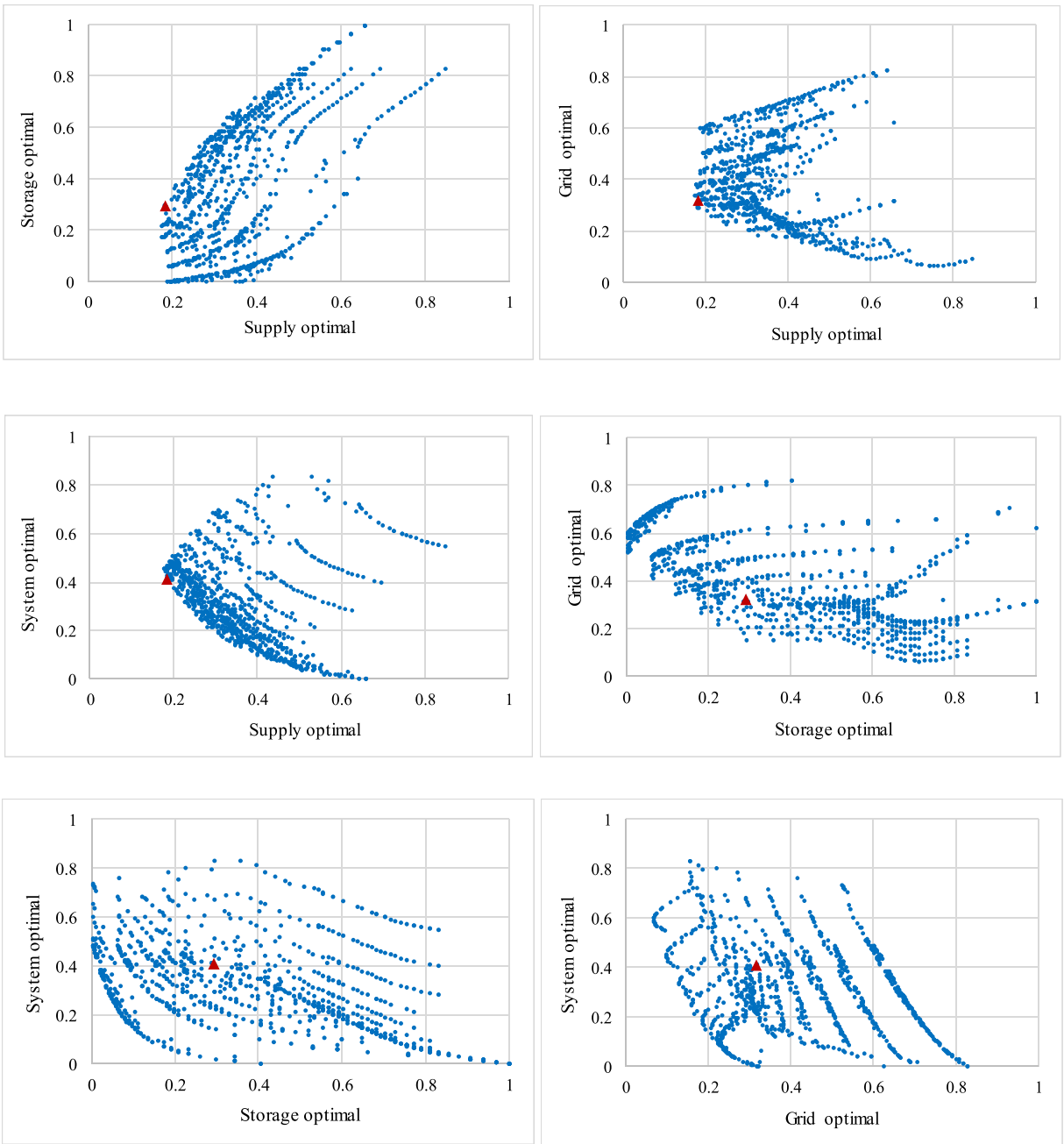

Fig. 6. Pareto-optimal solutions of the multi-criterion optimization case.

Please cite this article as: Liu J et al., Energy storage and management system design optimization for a photovoltaic integrated low-energy building, Energy, https://doi.org/10.1016/j.energy.2019.116424

is used by allocating the same weighting to corresponding objectives in these cases. In Case 7, all normalized criteria are subject to a multi-criterion optimization to find the final optimum solution determined by the minimum distance to the utopia point method [49]. And the optimization criteria of Case 3–7 are shown in Table 6.

3. Results and discussions

This section first summarizes the optimization results of studied cases when individual or combined optimization criteria on the system design and management are targeted. The PV-BES system performance in the four focused aspects i.e. energy supply, battery health, grid relief, and system economic-environmental impact, is then compared across studied cases to discuss the improvement potential of the novel energy management strategy. Furthermore, both local and global sensitivity analyses are conducted to identify the impact and significance of each design parameter.

Table 7 shows the targeted optimization criteria and corresponding design solutions of the studied cases. Case 1 is the existing case in the building under fixed grid electricity pricing without grid feed-in, treated as the baseline for comparison. Case 2 introduces time-of-use electricity pricing and allows grid feed-in from PV without limitations. Case 3–6 individually optimizes each aspect of the PV-BES system including the energy supply, battery storage, utility grid and whole system economic-environmental performance. Case 7 simultaneously optimizes technical, economic and environmental performances in all four aspects of the PV-BES system with a robust decision-making method.

The Pareto-optimal solutions in Case 7 are shown in Fig. 6, which demonstrates the trade-off among four major aspects including the energy supply, battery storage, utility grid and whole system. The final optimal solution highlighted as the red triangle is obtained using the decision-making strategy of the minimum distance to the utopia point [49].

3.1. Energy supply performance analysis

Figs. 7 and 8 show the power flow of the PV-BES system in the third week of June and December for Case 7. It shows that the building load generally exceeds the PV generation on typical weekdays in summer when the battery is discharged to meet the unsatisfied load during peak hours and charged by the utility grid during valley hours. The power flow in winter differs with that in summer as the building load is generally smaller with reduced air-conditioning load. Surplus PV power is then used to charge the battery and feed into the grid with a lower frequency of battery discharge.

In addition to introducing the hourly power flow of typical weeks in Case 7, the yearly results of three optimized energy supply indicators under the seven focused cases are also studied to make a comprehensive case comparison as shown in Fig. 9. Case 1 has the maximum annual average LCR, as the power from PV or battery is directed to meet the building load whenever available under the fixed grid pricing mode. However, Case 1 performs worst in SCR and EFF due to the strict limitation on grid import power. Compared with Case 1, EFF in Case 2 is increased by nearly 48.6% with the grid feed-in permission. Case 3 achieves the best overall performance in these three energy supply performance indicators as a result of the judicious mono-criterion optimization. Case 4 has the maximum SCR because battery charging by grid is controlled by a grid export limit of 0 kW and the battery can only be charged by PV. In addition, EFF varies between 0.430 and 0.504 as the grid import limit is not a significant factor for Case 4. SCR and EFF of Case 7 is increased by 15.0% and 48.6% than that of Case 1.

3.2. Battery health performance analysis

Fig. 10 compares battery cycling aging and SOH of studied cases. The annual cycling aging of the battery bank in Case 4 with the rated capacity at 120 kW h is the minimized by single-criterion optimization to about 0.027, leading to a high useable battery capacity of about 99.5% of its rated capacity after one-year operation. The calculated battery cycling aging is generally consistent with the result of an existing literature reporting a 0.124 cycling degradation of the lead-acid battery with the capacity of 165.6 kW h during four-year operation [36]. The maximum cycling aging is about 0.292 in Case 1 with a smaller battery number of 38 and

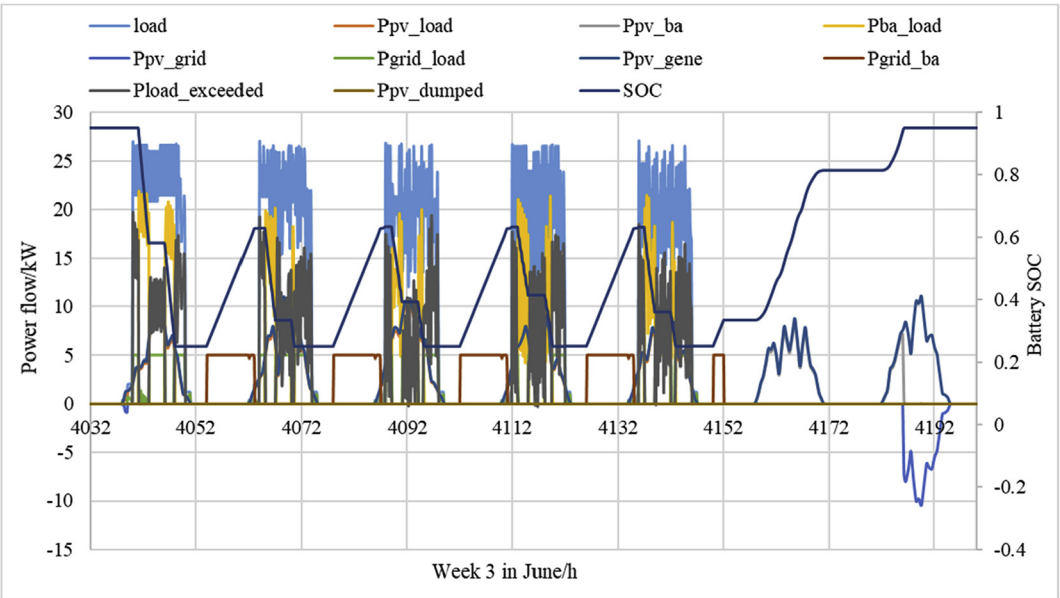

Fig. 7. Power flow in week 3 of June in Case 7.

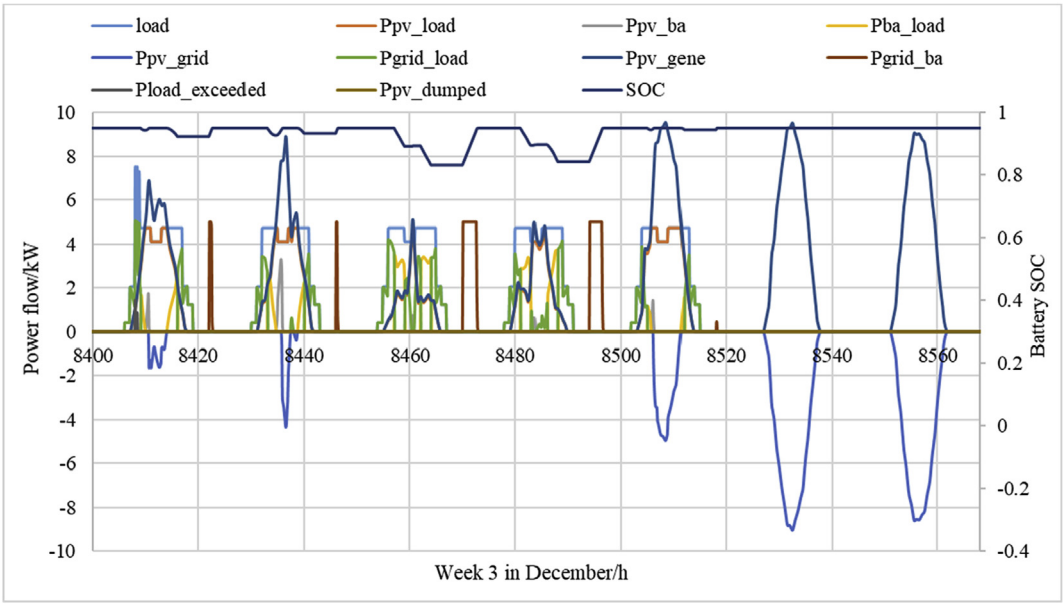

Fig. 8. Power flow in week 3 of December in Case 7.

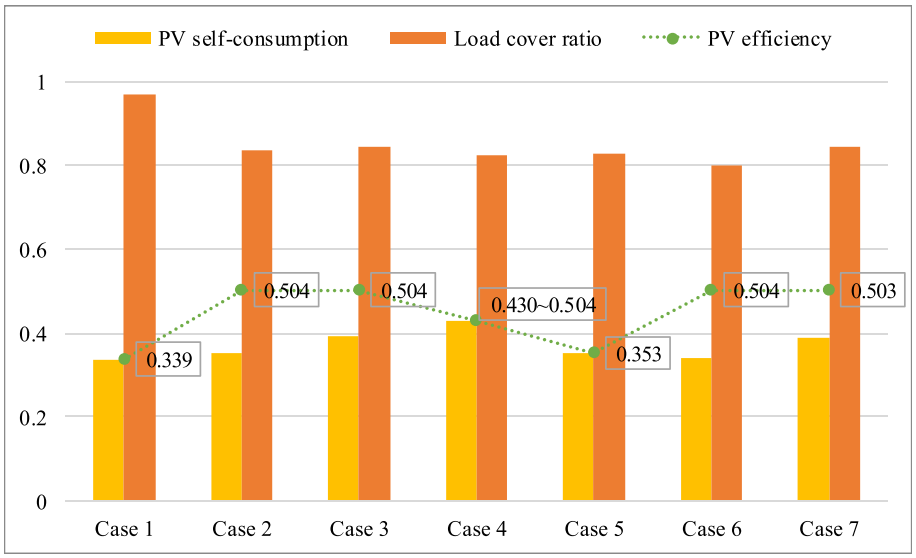

Fig. 9. Comparison of PV self-consumption, PV efficiency and load cover ratio of studied cases.

unrestricted battery charging. The annual battery cycling aging of Case 7 is smaller than that of Case 1 by 78.5%, resulting in the extension on the battery SOH from 94.2% in the baseline case to 98.7%. It is therefore proved significant to consider the battery health management in PV-BES systems and battery calendar aging will also be considered in the further work.

3.3. Grid relief performance analysis

Fig. 11 compares the annual STD of the net grid power and exceeded load of these studied cases. Case 5 achieves the minimum average grid stress among all cases with the lowest STD of about 4.60 under 28 battery cells and strict limitation for grid power import. The annual average exceeded load in Case 5 is 0 due to the high grid export limit. STD of net grid power in Case 6 reaches the maximum of about 5.68 with a minimum battery cell number and no grid import limitation. STD of net grid power in Case 4 changes from 4.72 to 5.05 given an optimized grid import limit ranging between 0 and 1, and STD of Case 7 is smaller than that of Case 1 by 3.4%.

The annual distribution of net grid power in the grid performance optimum case (Case 5) and multi-criterion optimization case (Case 7) is shown in Fig. 12 (a, b), where grid export power is presented by positive values and grid import power is in negative values. The flow distribution in Case 5 is more centralized than that in Case 7 with a smaller STD by about 6.5%. The cross section in yellow is the grid export limit optimized to be 30 kW in Case 5 and 5 kW in Case 7. The average load exceeding the grid export limit is determined to be 0 in Case 5 and 0.8 kW h/h in Case 7, as a useful reference for grid operators to maintain the network stability.

Please cite this article as: Liu J et al., Energy storage and management system design optimization for a photovoltaic integrated low-energy building, Energy, https://doi.org/10.1016/j.energy.2019.116424

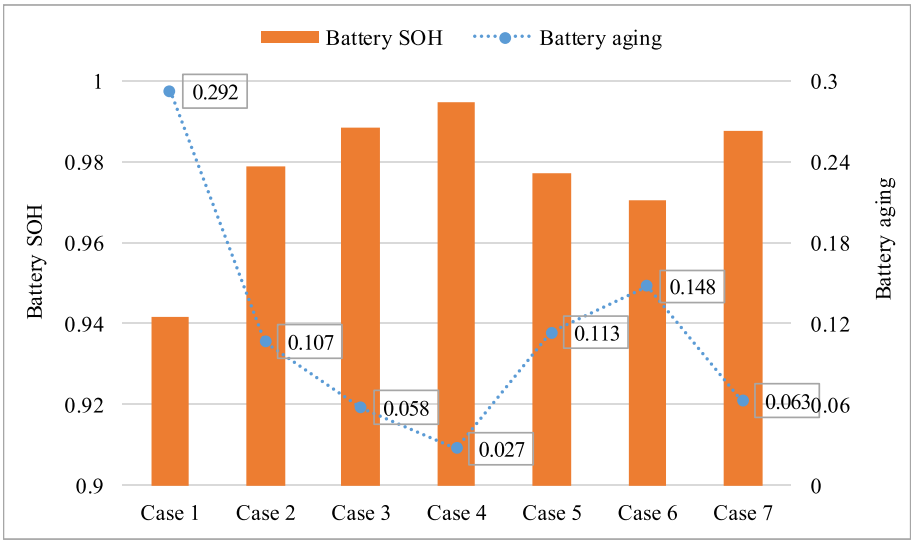

Fig. 10. Comparison of battery state of health and cycling aging of studied cases.

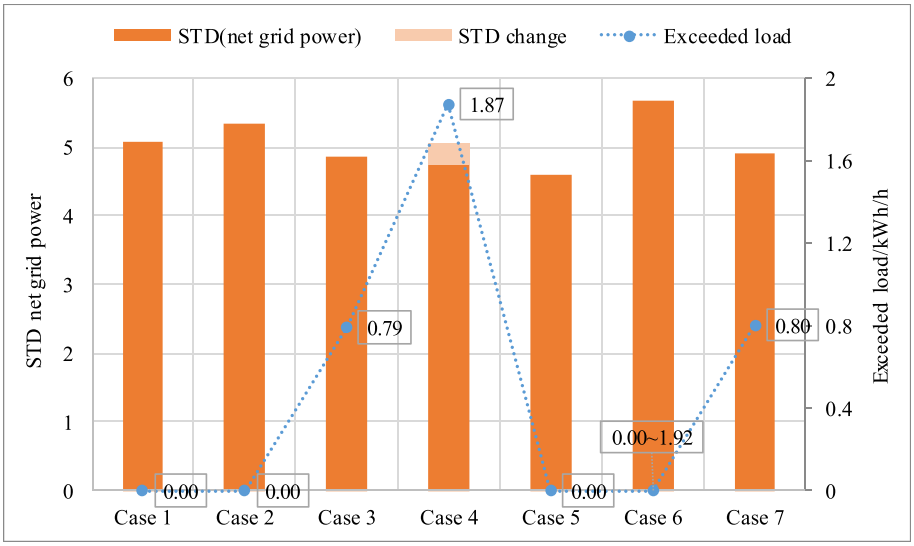

Fig. 11. Comparison of standard deviation of net grid power and exceeded load of studied cases.

3.4. System economic and environmental performance analysis

Fig. 13 compares NPV and LCOE of the PV-BES system including the initial cost, maintenance cost, electricity bill, RE subsidy and grid FIT within a 20-year operation. Case 6 has the minimum LCOE of about 0.124 $/kWh, which is lower than that of Case 1 of 0.170 $/kWh with a cost saving of nearly 26.8%. Case 4 has the maximum LCOE because of the high initial cost and electricity bill resulting from the large battery cell number and strict restriction on battery charging by the grid. Since the optimized grid import limit varies from 0 to 1 in Case 4, NPV of FIT changes from 0 to 2520 $ and LCOE ranges between 0.228 and 0.235 $/kWh. The calculated LCOE value agrees with the result reported in a previous literature indicating that LCOE of current PV-BES systems is around the range of 0.15–0.21 $/kWh [50].

A detailed breakdown of NPV and LCOE calculations for studied cases is summarized in Table 8. It reveals that simply adding the grid feed-in permission and time-of-use pricing control (Case 2) can bring 5100 $ reimbursement from the grid feed-in and save 3310 $ electricity bills compared with the existing operation case during the 20-year service time. As for Case 3 focusing on optimizing the energy supply performance, initial and maintenance costs are increased but the electricity bill is reduced and FIT is earned compared with the baseline case. When comparing Case 4 with the baseline case, LCOE is increased with the battery number rising from 38 to 100 while the battery is completely restricted from being charged by the grid. Case 5 has lower LCOE than the baseline case mainly due to lower initial and maintenance costs with less battery cells. Case 6 achieves best economic performance with a saving of about 16780 $ in total NPV and 0.046 $/kWh in LOCE. Case 7 has higher NPV and LCOE compared with the baseline case due to a balanced optimization of the energy supply, battery storage, utility grid and whole system covering technical, economic and environmental performances.

Fig. 14 compares the annual CO_2 emission of studied cases. The CO_2 emission in Case 1 and Case 5 is relatively high as the PV power is strictly restricted from feeding into the grid. Case 6 has the minimum annual CO_2 emission because of a full permission on grid

Please cite this article as: Liu J et al., Energy storage and management system design optimization for a photovoltaic integrated low-energy building, Energy, https://doi.org/10.1016/j.energy.2019.116424

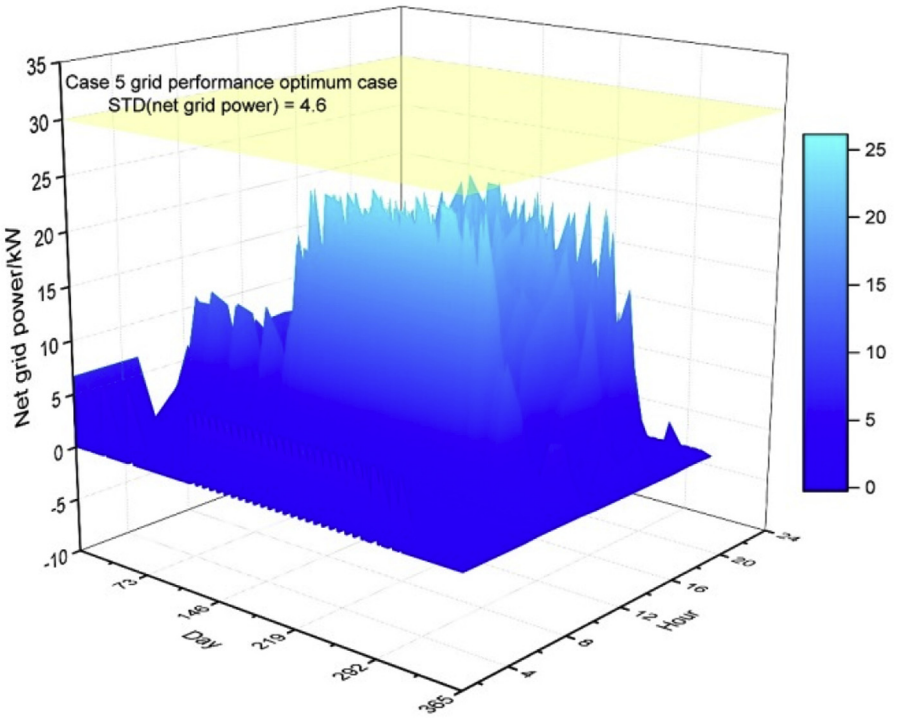

a

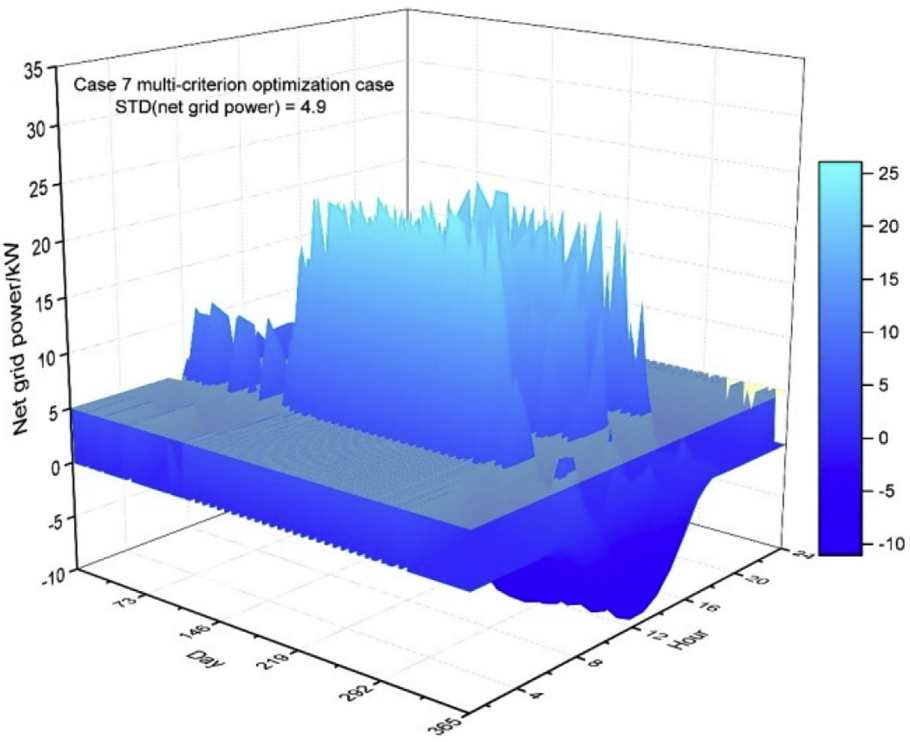

b

Fig. 12. (a) Annual net grid power flow in Case 5. (b) Annual net grid power flow in Case 7.

Please cite this article as: Liu J et al., Energy storage and management system design optimization for a photovoltaic integrated low-energy building, Energy, https://doi.org/10.1016/j.energy.2019.116424

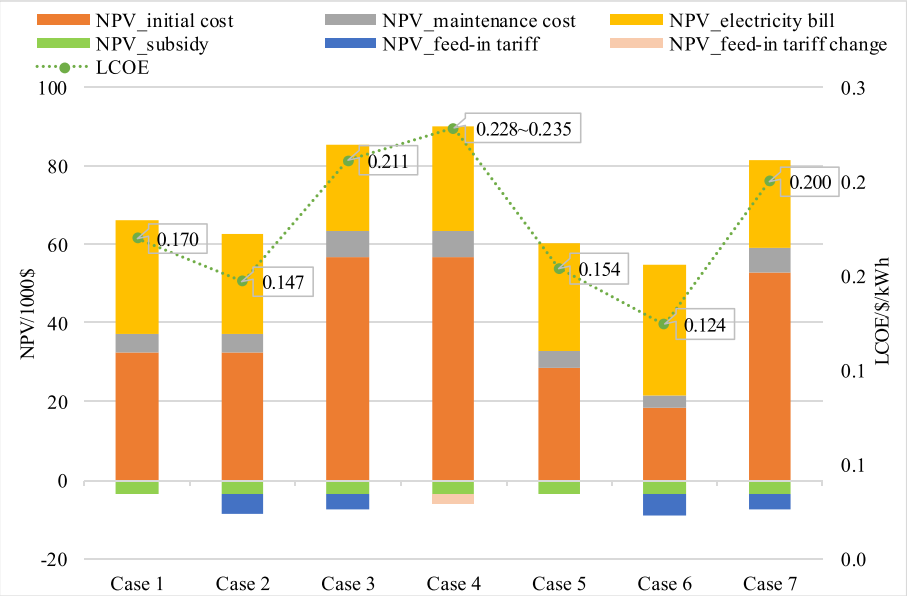

Fig. 13. Comparison of net present value and levelized cost of energy of studied cases.

Table 8
Economic comparison of studied cases.

Case	Case 1	Case 2	Case 3	Case 4	Case 5	Case 6	Case 7
	Existing in building	Grid feed-in and TOU	Supply optimal	Storage optimal	Grid optimal	System optimal	Overall optimal
Initial cost NPV/1000$	32.37	32.37	56.71	56.71	28.44	18.24	52.78
Maintenance cost NPV/1000$	4.70	4.70	6.78	6.78	4.36	3.49	6.44
Electricity bill NPV/1000$	29.03	25.72	21.75	26.73	27.42	33.10	22.07
Subsidy NPV/1000$	−3.37	−3.37	−3.37	−3.37	−3.37	−3.37	−3.37
FIT NPV/1000$	0.00	−5.10	−3.87	−2.52–0.00	0.00	−5.52	−4.01
Total NPV/1000$	62.72	54.31	77.99	84.32–86.84	56.85	45.94	73.91
Total NPV saving/1000$	_	8.41	−15.27	−21.60~-24.12	5.87	16.78	−11.19
LCOE/$/kWh	0.170	0.147	0.211	0.228–0.235	0.154	0.124	0.200
LCOE saving/$/kWh	_	0.023	−0.041	−0.058~-0.065	0.016	0.046	−0.030

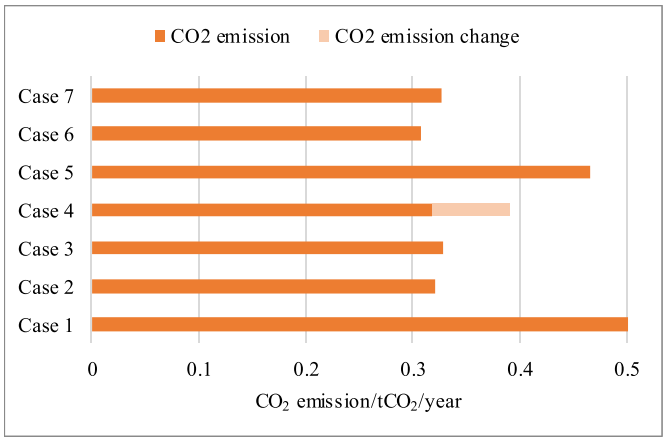

Fig. 14. Comparison of CO_2 emission of studied cases.

import power and less power loss in battery storage. The CO_2 emission in Case 7 is about 0.33 tCO_2/year, which is much lower than that of the baseline case (0.50 tCO_2/year) by nearly 34.7%.

3.5. Post-optimization sensitivity analysis

In order to further quantify the impact of system design and management parameters on different technical, environmental and economic performances of the PV-BES system, both local and global sensitivity analyses are conducted as future design references for relevant stakeholders of on-grid RE-EES systems in low-energy buildings.

3.5.1. Local sensitivity analysis

This part analyzes the sensitivity of optimization objectives by changing one design parameter at a time while keeping the other two fixed. The optimization result of Case 7 with the battery cell number at 90, grid export limit at 5 kW and grid import limit at 80% of rated PV power is taken as the reference. Fig. 15 shows the impact of the battery number on optimization objectives, and the optimization objectives are normalized for a clearer comparison. The battery cell number has a positive impact on SCR and LCR as more PV power can be utilized with increased storage capacity. The system LCOE and CO_2 emission also increase with the battery number due to a higher initial cost and higher battery charging loss. On the contrary, cycling aging of the battery bank, STD of net grid power and exceeded load are reduced with the increasing battery

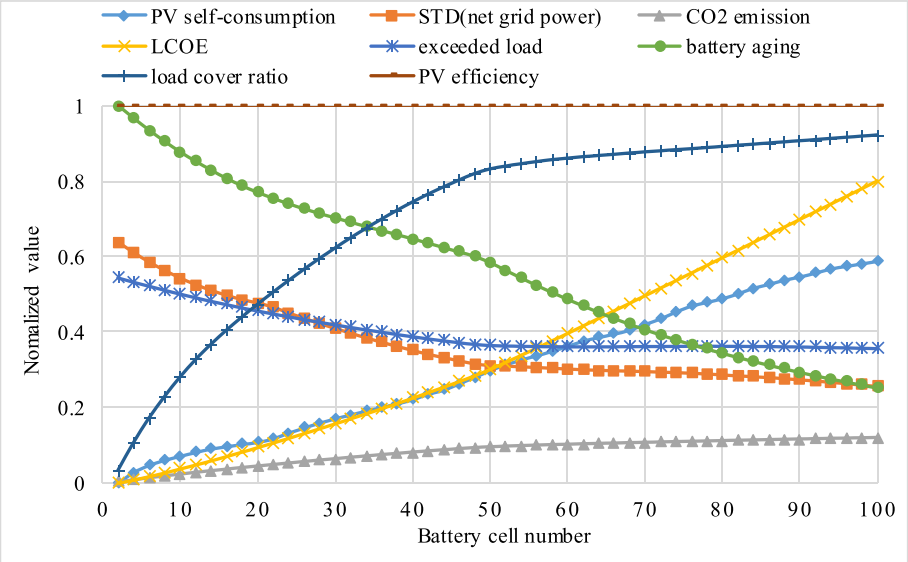

Fig. 15. Local sensitivity analysis of battery number on optimization objectives.

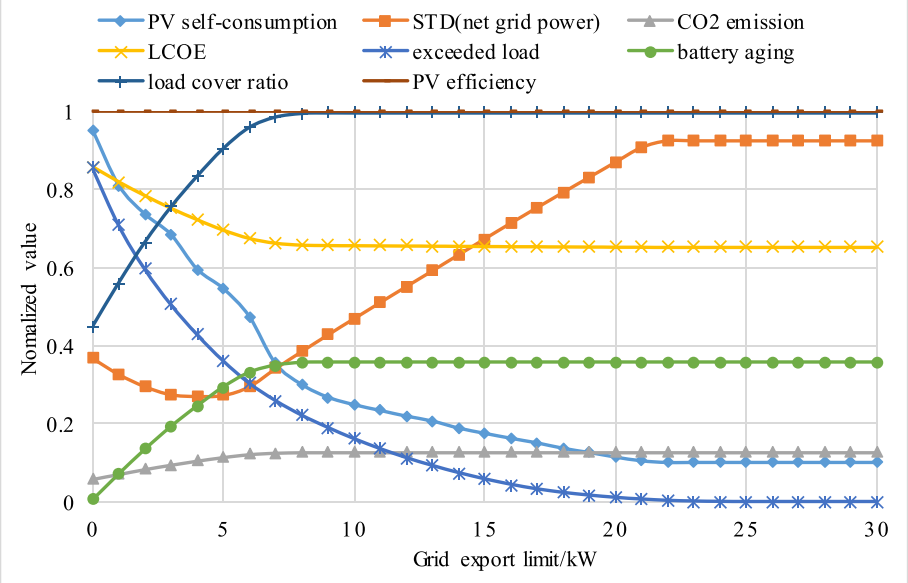

Fig. 16. Local sensitivity analysis of grid export limit on optimization objectives.

number and storage capacity.

Fig. 16 shows the impact of the grid export limit on normalized optimization objectives. LCR rises with the increasing grid export limit as more grid power is accessible to charge the battery which can meet the load in return. Higher grid export limits also result in a higher battery cycling aging and CO_2 emission while a lower SCR. Furthermore, the electricity bill is reduced due to an increased utilization of valley-price electricity. And the variation of these four objectives gradually levels off because the power flow from the battery bank to charge the load is directed after the PV supply. STD of net grid power shows a decreasing trend at the beginning and an increasing trend later with the rising grid export limit. A minimum STD is achieved when the limit is around 5 kW, which agrees well with the optimization result.

Fig. 17 shows the impact of the grid import limit (ratio of rated PV power) on normalized optimization objectives. The PV efficiency and STD of net grid power increase with the rising grid import limit as more surplus PV power can be delivered into the grid. The CO_2 emission and LCOE decrease with more grid import power because of the lower electricity bill and higher FIT. However, the grid import limit has a relatively small influence on SCR, EXR, battery aging and LCR. The exact impact of optimization parameters on these objectives is further explained by the global sensitivity analysis.

3.5.2. Global sensitivity analysis

To further validate the local sensitivity results and quantify the exact contribution of each design parameter, global sensitivity analyses based on FAST first-order indices [51] are conducted in this section. Fig. 18 shows the major impact of three design parameters on eight optimization objectives concerning the technical, economic and environmental performances of the PV-BES system. The

Please cite this article as: Liu J et al., Energy storage and management system design optimization for a photovoltaic integrated low-energy building, Energy, https://doi.org/10.1016/j.energy.2019.116424

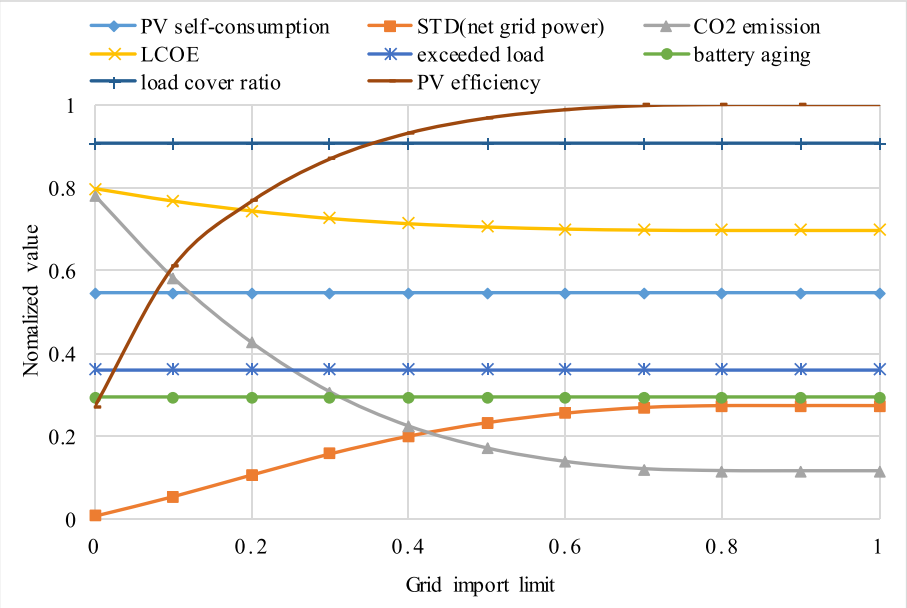

Fig. 17. Local sensitivity analysis of grid import limit on optimization objectives.

grid export limit has the major contribution of 50% to SCR variation, followed by the 23% contribution of the battery number. The grid import limit is identified to be not significant to SCR variation, and interactions of these three parameters account for 27% of the variation. Moreover, the grid export limit also accounts for 96% variation of the exceeded load. The battery number contributes to the major variation in LCOE, LCR and battery cycling aging for 95%, 83% and 77%, respectively. It can be found that the grid import limit has a major impact of 96% on the PV efficiency and CO_2 emission. The variation of the net grid power standard deviation is however comparatively evenly attributed to the grid import limit for 38%, the grid export limit for 27% and the battery number for 12%. It can be indicated that these three optimized parameters are significant to achieve a balanced optimum performance in technical, economic and environmental aspects of the PV-BES system. A suitable design of the energy storage and management system should consider both unique and interactive contributions from these parameters.

4. Conclusions

This study proposed a novel energy management control algorithm for the PV-BES system for a practical low-energy building in a typical hot summer and warm winter region of China. System design and management parameters are then subject to both single-criterion and multi-criterion optimizations based on the coupled TRNSYS and jEPlus + EA modeling platform with different decision-making approaches. The sensitivity of technical, economic and environmental system performance indicators to these optimization parameters are further investigated with robust local and global parametric analyses. Important conclusions are drawn as follows:

(1) A novel energy management strategy is proposed to improve the current operation condition of the PV-BES system without grid feed-in and time-of-use pricing (Case 1). The PV self-consumption and PV efficiency can be increased by 4.5% and 48.6% by introducing the grid import and peak-valley electricity pricing into the new control algorithm (Case 2). Battery cycling aging through the one-year operation can be reduced by 63.5%. The electricity bill NPV during the 20-year service time is reduced by 3310 $ with the 5100 $ income from the grid feed-in tariff, leading to the reduction of LCOE from 0.170 $/kWh to 0.147 $/kWh.

(2) Single-criterion optimization based design solutions are obtained for each performance criterion with the weighted sum method. The PV self-consumption, PV efficiency and load cover ratio can reach 0.39, 0.50 and 0.85 respectively with the optimum energy supply performance in Case 3. The annual battery cycling aging in the battery performance optimum case (Case 4) is about 0.027, and the battery SOH after one-year operation can be prolonged from 94.2% in the baseline case to 99.5%. Battery aging is proved crucial in the energy management and battery calendar aging should be studied in the further work. Remarkable impacts on relieving the utility grid can be achieved by setting the grid export limit and grid import limit (Case 5), where the standard deviation of net grid power can be reduced by 9.3% compared with the baseline case. The grid relief should therefore be considered in both design and operation stage of renewable energy systems. Total NPV and LCOE can be reduced by 16780 $ and 0.046 $/kWh in the whole system performance optimum case (Case 6), while the CO_2 emission can be reduced by 38.6% compared with the existing case in the target building. Cost and environmental impacts are also proved to be important in the energy management for a long-term operation.

(3) The optimum design configuration of the PV-BES system considering the simultaneous optimization of the energy supply, battery storage, utility grid and whole system for the target building is determined to be with 90 battery cells, a 5 kW grid export limit and 80% of rated PV power as the grid import limit. The minimum distance to the utopia point method is proved to be efficient and robust in determining the final optimum solution from the trade-off between different performance criteria. Compared with the baseline case, the PV self-consumption and PV efficiency can be increased by 15.0% and 48.6% respectively, while the standard deviation of net grid power, battery cycling aging and

Please cite this article as: Liu J et al., Energy storage and management system design optimization for a photovoltaic integrated low-energy building, Energy, https://doi.org/10.1016/j.energy.2019.116424

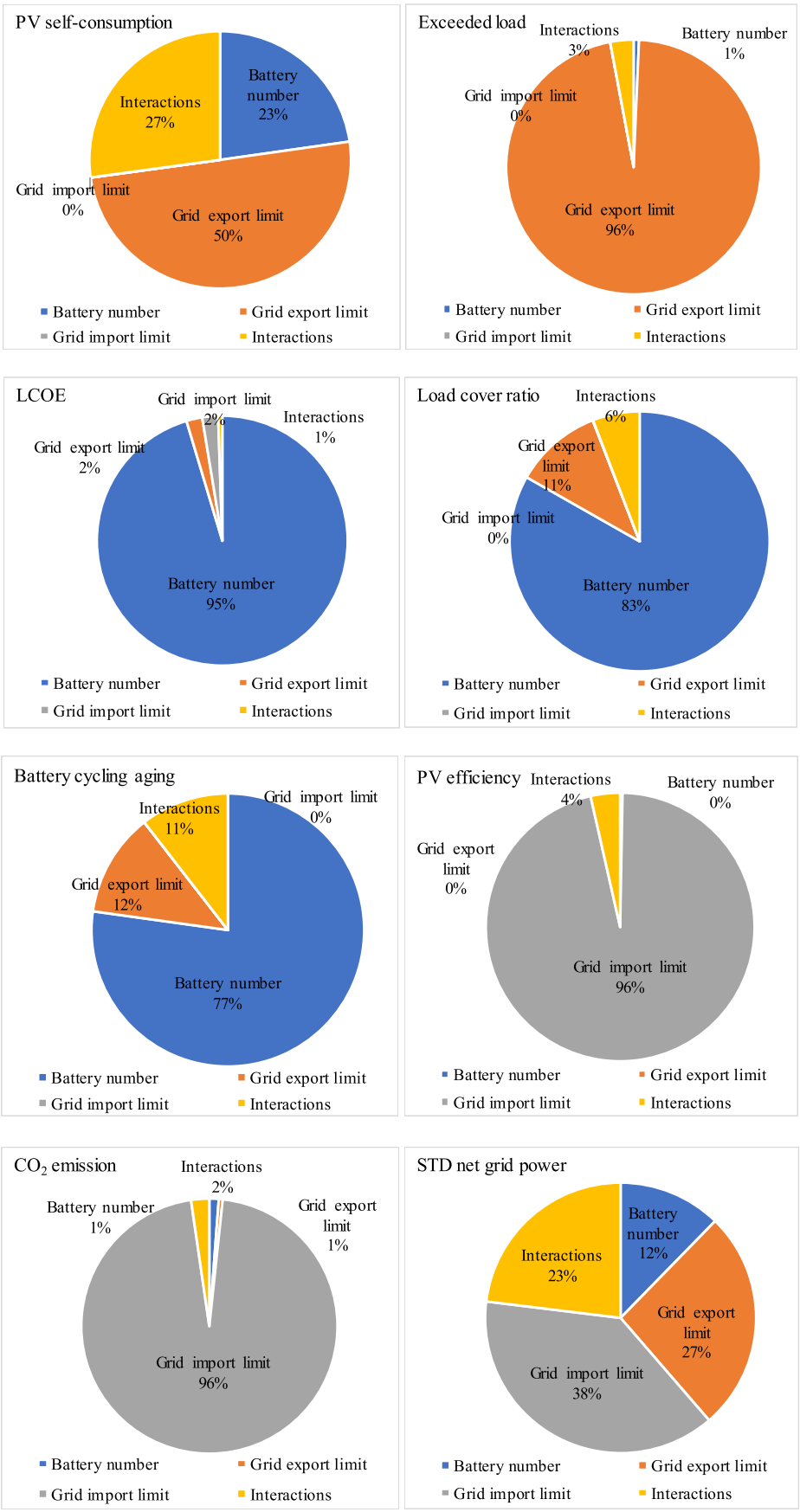

Fig. 18. Global sensitivity analysis of the optimization study.

Please cite this article as: Liu J et al., Energy storage and management system design optimization for a photovoltaic integrated low-energy building, Energy, https://doi.org/10.1016/j.energy.2019.116424

CO_2 emission is reduced by 3.4%, 78.5% and 34.7% respectively. A balance between technical, environmental and economic performance aspects has been achieved to deliver an overall optimum design and energy management solution.

(4) Both local and global sensitivity analyses are conducted to further quantify the unique and interactive impact of system design and management parameters on different performance indicators. The grid export limit has the major contribution to the PV self-consumption and exceeded load variation. The battery number contributes to the major variation in LCOE, load cover ratio and battery cycling aging. The grid import limit has a major impact on the PV efficiency and CO_2 emission. And the variation of the net grid power standard deviation is comparatively evenly attributed to these three optimization parameters. Findings from post-optimization sensitivity analyses can provide important references for the system design and management to further expand renewable energy applications in urban areas.

(5) Future work on RE-EES systems for power supply to low-energy buildings will be conducted considering following items: the demand control to integrate the building load; the combination of the photovoltaic-wind turbine hybrid generation and multi-energy storage technologies; scaling up the hybrid RE-EES system in building communities.

Acknowledgment

The work described in this paper was primarily supported by the PhD. studentship of The Hong Kong Polytechnic University. This work was also supported by the research project (1-ZE8B) of The Hong Kong Polytechnic University, China.

References

[1] REN21. Renewables 2019 global status report. 2019.
[2] International Energy Agency. Energy efficiency 2018: analysis and outlook to 2040. 2018.
[3] Solar Power Europe. Global market outlook for solar power. 2019. p. 2019–23.
[4] Global Wind Energy Council. Global wind report. 2018. 2019.
[5] Wang M, Peng J, Li N, Yang H, Wang C, Li X, et al. Comparison of energy performance between PV double skin facades and PV insulating glass units. Appl Energy 2017;194:148–60.
[6] Koskela J, Rautiainen A, Järventausta P. Using electrical energy storage in residential buildings – sizing of battery and photovoltaic panels based on electricity cost optimization. Appl Energy 2019;239:1175–89.
[7] Li C, Zhou D, Wang H, Cheng H, Li D. Feasibility assessment of a hybrid PV/diesel/battery power system for a housing estate in the severe cold zone—a case study of Harbin, China. Energy 2019;185:671–81.
[8] Paul Ayeng'o S, Axelsen H, Haberschusz D, Sauer DU. A model for direct-coupled PV systems with batteries depending on solar radiation, temperature and number of serial connected PV cells. Sol Energy 2019;183:120–31.
[9] Fina B, Auer H, Friedl W. Profitability of PV sharing in energy communities: use cases for different settlement patterns. Energy 2019;189:116148.
[10] Han X, Liang Y, Ai Y, Li J. Economic evaluation of a PV combined energy storage charging station based on cost estimation of second-use batteries. Energy 2018;165:326–39.
[11] Wang Z, Gu C, Li F. Flexible operation of shared energy storage at households to facilitate PV penetration. Renew Energy 2018;116:438–46.
[12] Gupta R, Bruce-Konuah A, Howard A. Achieving energy resilience through smart storage of solar electricity at dwelling and community level. Energy Build 2019;195:1–15.
[13] Sharma V, Haque MH, Aziz SM. Energy cost minimization for net zero energy homes through optimal sizing of battery storage system. Renew Energy 2019;141:278–86.
[14] Keiner D, Ram M, Barbosa LDSNS, Bogdanov D, Breyer C. Cost optimal self-consumption of PV prosumers with stationary batteries, heat pumps, thermal energy storage and electric vehicles across the world up to 2050. Sol Energy 2019;185:406–23.
[15] Hernández JC, Sanchez-Sutil F, Muñoz-Rodríguez FJ. Design criteria for the optimal sizing of a hybrid energy storage system in PV household-prosumers to maximize self-consumption and self-sufficiency. Energy 2019;186:115827.
[16] Liu J, Zhong C. An economic evaluation of the coordination between electric vehicle storage and distributed renewable energy. Energy 2019;186.
[17] Hernández JC, Sanchez-Sutil F, Vidal PG, Rus-Casas C. Primary frequency control and dynamic grid support for vehicle-to-grid in transmission systems. Int J Electr Power Energy Syst 2018;100:152–66.
[18] Sharma P, Kolhe M, Sharma A. Economic performance assessment of building integrated photovoltaic system with battery energy storage under grid constraints. Renew Energy 2019;145:1901–9.
[19] Komiyama R, Fujii Y. Optimal integration assessment of solar PV in Japan's electric power grid. Renew Energy 2019;139:1012–28.
[20] von Appen J, Braun M. Interdependencies between self-sufficiency preferences, techno-economic drivers for investment decisions and grid integration of residential PV storage systems. Appl Energy 2018;229:1140–51.
[21] Noor S, Yang W, Guo M, van Dam KH, Wang X. Energy Demand Side Management within micro-grid networks enhanced by blockchain. Appl Energy 2018;228:1385–98.
[22] O'Shaughnessy E, Cutler D, Ardani K, Margolis R. Solar plus: optimization of distributed solar PV through battery storage and dispatchable load in residential buildings. Appl Energy 2018;213:11–21.
[23] O'Shaughnessy E, Cutler D, Ardani K, Margolis R. Solar plus: a review of the end-user economics of solar PV integration with storage and load control in residential buildings. Appl Energy 2018;228:2165–75.
[24] Liang Z, Song Z, Wang J, Wang X, Zhang G. Three-stage scheduling scheme for hybrid energy storage systems to track scheduled feed-in PV power. Sol Energy 2019;188:1054–67.
[25] Bai B, Xiong S, Song B, Xiaoming M. Economic analysis of distributed solar photovoltaics with reused electric vehicle batteries as energy storage systems in China. Renew Sustain Energy Rev 2019;109:213–29.
[26] Al Essa MJM. Home energy management of thermostatically controlled loads and photovoltaic-battery systems. Energy 2019;176:742–52.
[27] Aktas A, Erhan K, Özdemir S, Özdemir E. Dynamic energy management for photovoltaic power system including hybrid energy storage in smart grid applications. Energy 2018;162:72–82.
[28] Wakui T, Sawada K, Yokoyama R, Aki H. Predictive management for energy supply networks using photovoltaics, heat pumps, and battery by two-stage stochastic programming and rule-based control. Energy 2019;179:1302–19.
[29] Ministry of Housing and Urban-Rural Construction of the People's Republic of China. Design standard for energy efficiency of public buildings. 2015.
[30] Cai J, Zhang H, Jin X. Aging-aware predictive control of PV-battery assets in buildings. Appl Energy 2019;236:478–88.
[31] Liu J, Chen X, Cao S, Yang H. Overview on hybrid solar photovoltaic-electrical energy storage technologies for power supply to buildings. Energy Convers Manag 2019;187:103–21.
[32] University of Wisconsin. TRNSYS 2017;18.
[33] National Renewable Energy Laboratory. Weather data sources.
[34] De Soto W, Klein SA, Beckman WA. Improvement and validation of a model for photovoltaic array performance. Sol Energy 2006;80(1):78–88.
[35] Duffie JA, Beckman WA, Worek W. Solar engineering of thermal processes. Wiley Online Library; 2013.
[36] Jiang Y, Kang L, Liu Y. A unified model to optimize configuration of battery energy storage systems with multiple types of batteries. Energy 2019;176:552–60.
[37] Hesse H, Martins R, Musilek P, Naumann M, Truong C, Jossen AJE. Economic optimization of component sizing for residential battery storage systems 2017;10(7):835.
[38] Voss K, Sartori I, Napolitano A, Geier S, Gonçalves H, Hall M, et al. Load matching and grid interaction of net zero energy buildings. EUROSUN 2010 International Conference on Solar Heating, Cooling and Buildings. 2010.
[39] Bertsch V, Geldermann J, Lühn T. What drives the profitability of household PV investments, self-consumption and self-sufficiency? Appl Energy 2017;204:1–15.
[40] National Development and Reform Commission. Notice of the national development and reform commission on improving the feed-in tariff mechanism for photovoltaic power generation. 2019.
[41] Bingham RD, Agelin-Chaab M, Rosen MA. Whole building optimization of a residential home with PV and battery storage in the Bahamas. Renew Energy 2019;132:1088–103.
[42] Magnor D, Sauer Dujep. Optimization of PV battery systems using genetic algorithmsvol. 99; 2016. p. 332–40.
[43] China Southern Power Grid. Industrial and commercial electricity price in Shen Zhen. 2019.
[44] Huang Z, Xie Z, Zhang C, Chan SH, Milewski J, Xie Y, et al. Modeling and multi-objective optimization of a stand-alone PV-hydrogen-retired EV battery hybrid energy system. Energy Convers Manag 2019;181:80–92.
[45] Lin WY, Lee WY, Hong TP. Adapting crossover and mutation rates in genetic algorithms. J Inf Sci Eng 2003;19(5):889–903.

Please cite this article as: Liu J et al., Energy storage and management system design optimization for a photovoltaic integrated low-energy building, Energy, https://doi.org/10.1016/j.energy.2019.116424

[46] Hamdy M, Nguyen A-T, Hensen JLM. A performance comparison of multi-objective optimization algorithms for solving nearly-zero-energy-building design problems. Energy Build 2016;121:57–71.
[47] Magnier L, Haghighat F. Multiobjective optimization of building design using TRNSYS simulations, genetic algorithm, and Artificial Neural Network. Build Environ 2010;45(3):739–46.
[48] Delgarm N, Sajadi B, Delgarm S, Kowsary F. A novel approach for the simulation-based optimization of the buildings energy consumption using NSGA-II: case study in Iran. Energy Build 2016;127:552–60.
[49] Chen X, Yang H, Sun K. A holistic passive design approach to optimize indoor environmental quality of a typical residential building in Hong Kong. Energy 2016;113:267–81.
[50] Chaianong A, Bangviwat A, Menke C, Breitschopf B, Eichhammer W. Customer economics of residential PV–battery systems in Thailand. Renew Energy 2020;146:297–308.
[51] Chen X, Yang H, Peng J. Energy optimization of high-rise commercial buildings integrated with photovoltaic facades in urban context. Energy 2019;172:1–17.

Please cite this article as: Liu J et al., Energy storage and management system design optimization for a photovoltaic integrated low-energy building, Energy, https://doi.org/10.1016/j.energy.2019.116424